Electron transport properties of carbon nanotube–graphene contacts

Brandon G. Cook,[1] William R. French,[2] and Kálmán Varga[1]
[1]*Department of Physics and Astronomy, Vanderbilt University, Nashville, Tennessee 37235, USA*
[2]*Department of Chemical and Biomolecular Engineering, Vanderbilt University, Nashville, Tennessee 37235, USA*

(Received 14 May 2012; accepted 2 August 2012; published online 8 October 2012)

The properties of carbon nanotube-graphene junctions are investigated with first-principles electronic structure and electron transport calculations. Contact properties are found to be key factors in determining the performance of nanotube based electronic devices. In a typical single-walled carbon nanotube-metal junction, there is a p-type Schottky barrier of up to ~0.4 eV which depends on the nanotube diameter. Calculations of the Schottky barrier height in carbon nanotube-graphene contacts indicate that low barriers of 0.09 eV and 0.04 eV are present in nanotube-graphene contacts ((8,0) and (10,0) nanotubes, respectively). Junctions with a finite contact region are investigated with simulations of the current-voltage characteristics. The results suggest the suitability of the junctions for applications and provide insight to explain recent experimental findings. © *2012 American Institute of Physics*. [http://dx.doi.org/10.1063/1.4756693]

Carbon nanotubes (CNTs) and graphene have attracted a lot of attention because of their unique electrical, optical, thermal, and mechanical properties.[1–4] Graphene has very large electron mobility at room temperature[5] and is easy to fabricate on a wafer scale,[6,7] but does not possess a band gap.[5] This makes it challenging to create graphene-based transistors with the large on/off ratios, which are required for logic applications.[8] While CNTs have a useful large energy gap allowing fabrication of transistors with large on/off ratios, the performance of these transistors crucially depends on the contacts between the CNT and the electrodes.[1–4] All-carbon hybrid architectures suited for applications are possible through the combination of advantageous material properties of graphene and nanotubes. For example, a highly efficient all-carbon solar cell could be constructed by combining CNTs to efficiently generate electron-hole pairs[9] with transparent conductive graphene electrodes.[10–13]

A long standing issue for CNT and graphene based electronics has been the quality of contacts with electrode materials such as Pd, Ti, or Al.[14–17] A common feature of the CNT-metal contacts has been the presence of a Schottky barrier at the nanotube-metal interface.[18,19] The Schottky barriers severely limit transistor conductance in the "ON" state, and reduce the current delivery capability—a key factor of device performance. High work-function metal (e.g., Pd) contacts have reduced the Schottky barrier providing nearly ohmic contacts to single-walled CNTs[1,16,20] and enabled room-temperature conductance near the ballistic transport limit. Generally, it is found that Pd has a negligible Schottky barrier height (SBH) when nanotubes have a diameter larger than ~1.4 nm, and that smaller nanotubes such as the (8,0) (diameter ~0.62 nm) have barriers of up to ~0.4 eV, depending on diameter. The SBH at CNT-metal contacts has also been previously studied with first-principles calculations.[21–25] It is found that the SBH depends strongly on the atomic details of the system, and in agreement with the experimental findings, the Ti and Pd(100) contacts have the lowest SBH.

While the properties of graphene or CNT in contact with common electrode metals has been investigated,[1,16,20–25] junctions between the two materials have been the subject of only a few studies. Pei *et al.*[26] recently presented measurements with few layer graphene and large nanotubes (diameter unspecified). They conclude that graphene is an unsuitable electrode material for use in transistor devices based on the few devices they measured. However, it should be noted that detailed analysis of the contact geometry is lacking and it is well known that work function of graphene depends on the number of layers.[27] Another group has demonstrated that the inclusion of a graphitic interface layer improved electronic characteristics in single wall CNT devices.[28] It has also been shown that contact resistance between graphite and multiwalled CNTs can be tuned by controlling the contact geometry.[29]

In this report, we investigate the contact properties of graphene-CNT interfaces with first-principles calculations. The p-type SBH is calculated for semiconducting (8,0) and (10,0) nanotubes on graphene surfaces with the potential profile lineup method.[21,30] These calculations correspond to the limit of an extended clean contact region between graphene and a long CNT. With this model, we show that the SBH is low compared to that found in Pd-CNT contacts. Simulations with a finite contact region show the role of contact region length and edge effects in determining the electrical properties. Particularly showing that the nanotube chirality is the primary factor. The electron transmission curves are calculated and current-voltage characteristics for (8,0) and (10,0) CNTs in contact with graphene with different length of overlap of graphene and CNTs in the scattering region are presented. We conclude by discussing the implications of our results in terms of recent experiments.

Two types of geometries are used in this work: a "device" geometry with a carbon nanotube connected to a graphene lead (see Figure 1) and an "ideal" contact geometry where a carbon nanotube sits atop a graphene sheet in a periodic cell (see Figure 2). Different methods were used to obtain optimized coordinates in each case. In the "ideal" case, the total energy is minimized by optimizing a number of geometric factors such as rotation of the nanotube, nanotube–graphene distance, and translation of the nanotube with

 © 2012 American Institute of Physics

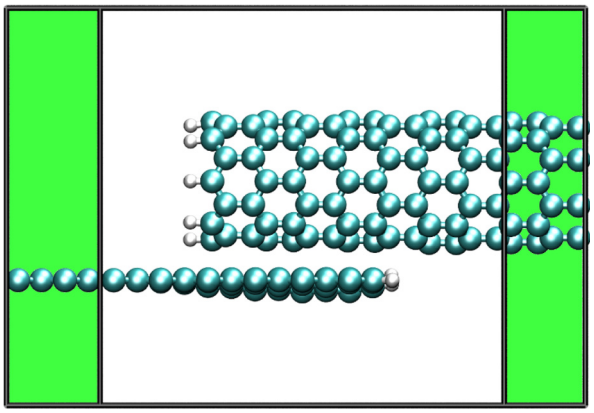

FIG. 1. Graphene-carbon nanotube device. The nanotube is (8,0) and the graphene is aligned along the zigzag direction with an overlap region of 10 Å. The boxes indicate scattering and electrode regions with the electrode regions highlighted in green.

respect to the graphene. Following this, an unconstrained optimization is done until all forces are less than 0.01 eV/Å. This approach is used to avoid local minima in the energy landscape. All calculations for this geometry are done with density functional theory (DFT) as implemented in VASP.[31] Projected augmented waves are used to represent core electrons, and the local density approximation is used for exchange and correlation. The Brilloiun zone is sampled by 15 points along the nanotube axis generated with the Monkhorst-Pack method. A planewave cutoff energy of 400 eV was used. In the other case of the "device" geometry, a different procedure is used due to the large cell size, large number of atoms and the non-periodic nature of the geometry. A code based on planewaves is more suitable for smaller systems with periodic simulation cells and is impractical for application to large non-periodic systems which contain large amounts of vacuum. We use the TranSIESTA[32] code with a szp basis set and a grid spacing which corresponds to a 490 eV planewave cutoff energy. We note that similar accuracy is achieved in carbon based systems with both codes. As in the "ideal" case, factors such as nanotube rotation and graphene–nanotube distance were optimized first. Then coordinates are optimized until all forces are less than 0.05 eV/Å. The electrode Brilloiun zones were sampled with a 3×25 grid of kpoints generated by the Monkhorst-Pack method.

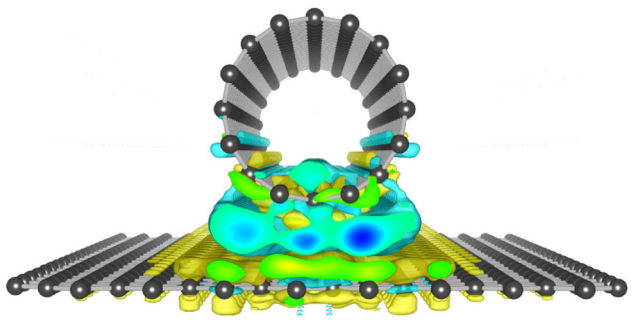

FIG. 2. Charge transfer between graphene and an (8,0) nanotube. Self-consistent density is obtained for the case of the nanotube far away from the graphene and the case of the graphene and nanotube separated by $d \approx 3.0$ Å. The system is periodic along the nanotube axis. Blue indicates an excess of charge and yellow a depletion.

The self-consistent calculation of the scattering region is done with 3 tranverse kpoints. Electron transmission probability curves are generated with 31 transverse kpoints to obtain converged values.

The potential profile lineup method has been used to study the Schottky barrier between metal and semiconductor.[30] We adopt a similar approach that has been used to study CNT-metal junctions.[21,22] The difference between the Fermi level of the combined system and valence band edge of the semiconductor is the p-type Schottky barrier,

$$\Delta_p = E_F - E_V, \tag{1}$$

where E_F is the Fermi level of the combined graphene-nanotube system and E_V is valence band edge of the nanotube. The SBH, Δ_p, can be determined by comparing features of the metal/semiconductor combined system to those of the pure semiconductor system by rewriting Eq. (1) as

$$\Delta_p = (E_F - \langle V_1 \rangle_{\mathrm{CNT}}) - (E_V - \langle V_2 \rangle_{\mathrm{CNT}}). \tag{2}$$

We have introduced $\langle V \rangle$ to indicate the average potential at an atomic core. The atomic core potential is used to line up the energy levels of the nanotube-only calculation and the combined graphene-nanotube calculation. In the calculation, E_F and $\langle V_1 \rangle$ are taken from the combined system and $\langle V_1 \rangle$ is evaluated only with the carbon atoms, which are furthest from the graphene. This is done to reduce error associated with charge transfer, which is limited to the interface region as confirmed by a Bader analysis.[33] The valence band edge E_V and $\langle V_2 \rangle$ are taken from a calculation with a nanotube only. In this case, with only the nanotube in the simulation cell the average is done over all atoms in the nanotube.

With this approach, we calculate the p-type Schottky barrier heights for (8,0) and (10,0) nanotubes with calculated band gaps of 0.55 eV and 0.80 eV, respectively. These nanotubes are the smallest "big gap" semiconducting nanotubes with diameters of ~0.62 nm and ~0.78 nm. Experiments report values of 0.95 to 0.65 eV for nanotubes with diameters from 0.7 to 1.0 nm.[34] A SBH of 0.09 eV was found in the (8,0) case and 0.04 eV was found in the (10,0) case. These results are summarized in Table I. This is in contrast to the measured value of $\Delta_p \approx 0.4$ eV in Pd-CNT junctions.[15] The redisitribution of charge between the graphene and CNT is shown in Figure 2, indicating the formation of bonds. The low Schottky barrier can be attributed to the similar work function of graphene and CNT and the quality of contact in the calculation. Measurements done with multi-layer graphene (with a varying workfunction[27]) and unclear contact quality that show the presence of barriers[26] can be attributed to these factors. This conclusion is supported by measurements, where a graphitic layer surrounds the nanotube and

TABLE I. Properties of nanotubes: E_b is the calculated band gap, d is the nanotube diameter, and Δ_p is the p-type Schottky barrier.

Nanotube	E_b (eV)	d (nm)	Δ_p (eV)
(8,0)	0.55	0.63	0.09
(10,0)	0.80	0.78	0.04

improved characteristics such as higher "ON" currents are observed after an annealing process.[28]

To compliment the calculation of the SBH, we investigate the current-voltage (IV) characteristics of CNT-graphene junctions with (8,0) and (10,0) nanotubes. The calculation is done within the NEGF-DFT formalism as implemented in the TranSIESTA code.[32] For each nanotube, we use two different lengths of overlap region between the CNT and graphene electrode, namely, 5 Å and 10 Å. The graphene electrodes are aligned along the zigzag direction. Some general trends can be observed in the computed IV characteristics (see Figure 3). Increasing the length of the overlap region between the carbon nanotube and graphene decreases the transport gap toward the value expected for just the nanotube alone. This suggests that the influence of edge effects is decreased as the overlap region is extended. The size of transport gap depends also on the CNT—the nanotube with the larger band gap, the (10,0) has a larger transport gap. These points indicate that the characteristics of junctions depend strongly on the specific nanotube employed. We also note that the profile of the IV curve differs between nanotubes: junctions with (8,0) nanotubes show a small initial increase in current followed by a sharper increase at high voltages, while the (10,0) nanotubes show a single sharp increase in current. In the high bias regions, the current obtains high values on the order of 20 μA, which is roughly the electron-phonon interaction limited value in singe-wall nanotubes that are longer than the electron mean free path.[35] One can then expect that in a clean interface between a carbon nanotube and graphene, the interface will not be the limiting factor.

In conclusion, we have studied the electronic properties of CNT-graphene contacts. First, we showed that the p-type Schottky barrier is low in very long ideal junctions with (8,0) and (10,0) nanotubes. Values for the SBH of 0.09 eV and 0.04 eV were found for the (8,0) and (10,0) cases, respectively. These are significantly lower than the reported values for Pd of $\Delta_p \approx 0.3 - 0.4$ eV. To further investigate the transport properties, we calculated the current-voltage response of (8,0) and (10,0) nanotubes in contact with graphene. We varied the length of the contact region and found that the chirality of the nanotube is the important factor. These calculations provide qualitative insight into the role of the junctions in determining the IV characteristics. Recent experiments offer conflicting opinions on the suitability of graphitic carbon contacts for applications, such as transistors. Our results indicate that the contacts are suitable and suggest that an experiment with single-wall nanotubes contacting suspended graphene may be required to diminish substrate effects.

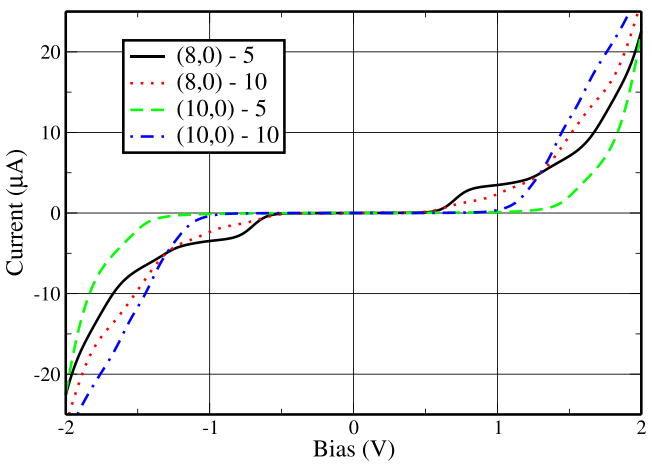

FIG. 3. Calculated current-voltage response for various CNT-graphene junctions. The low-bias transmission spectrum is integrated to obtain the IV curves. Curves with (8,0) and (10,0) nanotubes with a 5 Å and 10 Å of overlap with the graphene are shown (see Figure 1).

[1]J. Kong, E. Yenilmez, T. W. Tombler, W. Kim, H. Dai, R. B. Laughlin, L. Liu, C. S. Jayanthi, and S. Y. Wu, Phys. Rev. Lett. **87**, 106801 (2001).
[2]D. Mann, A. Javey, J. Kong, Q. Wang, and H. Dai, Nano Lett. **3**, 1541 (2003).
[3]A. Javey, J. Guo, D. B. Farmer, Q. Wang, D. Wang, R. G. Gordon, M. Lundstrom, and H. Dai, Nano Lett. **4**, 447 (2004).
[4]S. Rosenblatt, Y. Yaish, J. Park, J. Gore, V. Sazonova, and P. L. McEuen, Nano Lett. **2**, 869 (2002).
[5]A. K. Geim and K. S. Novoselov, Nature Mater. **6**, 183 (2007).
[6]K. S. Kim, Y. Zhao, H. Jang, S. Y. Lee, J. M. Kim, K. S. Kim, J.-H. Ahn, P. Kim, J.-Y. Choi, and B. H. Hong, Nature **457**, 706 (2009).
[7]S. Bae, H. Kim, Y. Lee, X. Xu, J.-S. Park, Y. Zheng, J. Balakrishnan, T. Lei, H. Ri Kim, Y. I. Song, Y.-J. Kim, K. S. Kim, B. Ozyilmaz, J.-H. Ahn, B. H. Hong, and S. Iijima, Nat. Nanotechnol. **5**, 574 (2010).
[8]A. Bachtold, P. Hadley, T. Nakanishi, and C. Dekker, Science **294**, 1317 (2001).
[9]N. M. Gabor, Z. Zhong, K. Bosnick, J. Park, and P. L. McEuen, Science **325**, 1367 (2009).
[10]X. Wang, L. Zhi, and K. Mullen, Nano Lett. **8**, 323 (2008).
[11]J. Wu, H. A. Becerril, Z. Bao, Z. Liu, Y. Chen, and P. Peumans, Appl. Phys. Lett. **92**, 263302 (2008).
[12]G. Eda, Y.-Y. Lin, S. Miller, C.-W. Chen, W.-F. Su, and M. Chhowalla, Appl. Phys. Lett. **92**, 233305 (2008).
[13]V. C. Tung, L.-M. Chen, M. J. Allen, J. K. Wassei, K. Nelson, R. B. Kaner, and Y. Yang, Nano Lett. **9**, 1949 (2009).
[14]G. Giovannetti, P. A. Khomyakov, G. Brocks, V. M. Karpan, J. van den Brink, and P. J. Kelly, Phys. Rev. Lett. **101**, 026803 (2008).
[15]Z. Chen, J. Appenzeller, J. Knoch, Y.-M. Lin, and P. Avouris, Nano Lett. **5**, 1497 (2005).
[16]W. Liang, M. Bockrath, D. Bozovic, J. H. Hafner, M. Tinkham, and H. Park, Nature **411**, 665 (2001).
[17]Z. Zhang, X. Liang, S. Wang, K. Yao, Y. Hu, Y. Zhu, Q. Chen, W. Zhou, Y. Li, Y. Yao, J. Zhang, and L.-M. Peng, Nano Lett. **7**, 3603 (2007).
[18]S. Heinze, J. Tersoff, R. Martel, V. Derycke, J. Appenzeller, and P. Avouris, Phys. Rev. Lett. **89**, 106801 (2002).
[19]J. Appenzeller, J. Knoch, V. Derycke, R. Martel, S. Wind, and P. Avouris, Phys. Rev. Lett. **89**, 126801 (2002).
[20]A. Javey, J. Guo, Q. Wang, M. Lundstrom, and H. Dai, Nature **424**, 654 (2003).
[21]B. Shan and K. Cho, Phys. Rev. B **70**, 233405 (2004).
[22]W. Zhu and E. Kaxiras, Appl. Phys. Lett. **89**, 243107 (2006).
[23]Y. He, J. Zhang, S. Hou, Y. Wang, and Z. Yu, Appl. Phys. Lett. **94**, 093107 (2009).
[24]Y. Matsuda, W.-Q. Deng, and W. A. Goddard, J. Phys. Chem. C **114**, 17845 (2010).
[25]F. Lonard and D. A. Stewart, Nanotechnology **17**, 4699 (2006).
[26]T. Pei, H. Xu, Z. Zhang, Z. Wang, Y. Liu, Y. Li, S. Wang, and L.-M. Peng, Appl. Phys. Lett. **99**, 113102 (2011).
[27]H. Hibino, H. Kageshima, M. Kotsugi, F. Maeda, F.-Z. Guo, and Y. Watanabe, Phys. Rev. B **79**, 125437 (2009).
[28]Y. Chai, A. Hazeghi, K. Takei, H.-Y. Chen, P. Chan, A. Javey, and H.-S. Wong, IEEE Trans. Electron Devices **59**, 12 (2012).
[29]S. Paulson, A. Helser, M. B. Nardelli, R. M. Taylor, M. Falvo, R. Superfine, and S. Washburn, Science **290**, 1742 (2000).
[30]R. Dandrea and C. Duke, J. Vac. Sci. Technol. A **11**, 848 (1993).
[31]G. Kresse and J. Hafner, Phys. Rev. B **47**, 558 (1993).
[32]K. Stokbro, J. Taylor, M. Brandbyge, and P. Ordejón, Ann. N. Y. Acad. Sci. **1006**, 212 (2003).
[33]W. Tang, E. Sanville, and G. Henkelman, J. Phys.: Condens. Matter **21**, 084204 (2009).
[34]T. Odom, J. Huang, P. Kim, and C. Lieber, Nature **391**, 62 (1998).
[35]Z. Yao, C. L. Kane, and C. Dekker, Phys. Rev. Lett. **84**, 2941 (2000).